Four decades of water quality change in the upper San Francisco Estuary

Marcus W. Beck[1]*, **Thomas W. Jabusch**[2], **Philip R. Trowbridge**[2], **David B. Senn**[2]

Corresponding author: marcusb@sccwrp.org

[1]*USEPA National Health and Environmental Effects Research Laboratory*
Gulf Ecology Division, 1 Sabine Island Drive, Gulf Breeze, FL 32561

Current address: Southern California Coastal Water Research Project
3535 Harbor Blvd, Suite 110, Costa Mesa, CA 92626

[2]*San Francisco Estuary Institute*
4911 Central Ave, Richmond, CA 94804

Version Date: Fri Oct 20 10:57:35 2017 -0700

Abstract

Quantitative descriptions of water quality, physical, and biological characteristics in estuaries is critical for developing an ecological understanding of drivers of change. Historical trends and relationships between key species of dissolved inorganic nitrogen (ammonium, nitrate/nitrite, total) from the Delta region of the San Francisco Estuary (SFE) were modeled with an estuarine adaptation of the Weighted Regressions on Time, Discharge, and Season (WRTDS). Trend analysis with flow-normalized results demonstrated the potential to interpret different changes relative to observed data that included flow effects, such that several trends with flow-normalized data had changes in magnitude and even reversal of trends relative to the observed. We further described mechanisms of change with two case studies that evaluated 1) downstream changes in nitrogen following upgrades at a wastewater treatment plant, and 2) interactions between biological invaders, chlorophyll, and flow in Suisun Bay. WRTDS results for ammonium trends showed a distinct signal as a result of upstream wastewater treatment plant (WWTP) upgrades, with specific reductions observed in the winter months during low-flow conditions. Results for Suisun Bay showed that chlorophyll *a* (chl-*a*) production in early years was directly stimulated by flow, whereas the relationship with flow in later years was indirect and influenced by grazing pressure. Although these trends and potential causes of change have been described in the literature, results from WRTDS provided an approach to test alternative hypotheses of spatiotemporal drivers of nutrient dynamics in the Delta.

1   Introduction

Understanding drivers of water quality changes in large estuaries depends on accurate descriptions of source inputs from the watershed. The Sacramento - San Joaquin River Delta (hereafter 'Delta') is a mosaic of inflows in the upper San Francisco Estuary (SFE) that receives and processes inputs from the highly agricultural watershed of the Central Valley (Jassby and Cloern 2000, Jassby et al. 2002, Jassby 2008). Sediment transport and wastewater treatment plant (WWTP) inputs from the Delta are primary sources of nutrients for the estuary (Dugdale et al. 2007, Cornwell et al. 2014). Although water quality conditions in SFE symptomatic of eutrophication have historically been infrequent, changes in response to stressors suggests that recent conditions have not followed past trajectories. Increases in phytoplankton biomass, reductions in dissolved oxygen, and increasing abundance of species associated with harmful algal blooms (e.g., *Pseudo-nitzschia*, *Alexandrium*, *Dinophysis spp.*) have been a recent concern for the management of this prominent system (Lehman et al. 2005, Cloern et al. 2005, 2007, Shellenbarger et al. 2008). As a result, chlorophyll *a* (chl-*a*) thresholds to assess and manage levels of concern for phytoplankton biomass in the lower estuary have been proposed (Sutula et al. 2017). Although these changes are linked to drivers at different spatial and temporal scales, describing inputs from the Delta is critical to understand downstream effects.

Rates of primary production in coastal habitats are often defined by nutrient concentrations, although a simple relationship between enrichment and water quality changes can be difficult to determine (Cloern 2001). Nutrient concentrations are generally non-limiting for phytoplankton growth in the upper SFE. In contrast, light conditions have long been considered the primary limiting factor preventing accumulation of phytoplankton biomass (Cole and Cloern

1984, Alpine and Cloern 1988), whereas grazing pressure from pelagic fishes and benthic

invertebrates can reduce phytoplankton during periods of growth (Nichols 1985, Jassby 2008,

Kimmerer and Thompson 2014). Moreover, changes in flow management practices compounded

with climate variation have altered flushing rates and turbidity as key factors that moderate

phytoplankton growth in the system (Alpine and Cloern 1992, Lehman 2000, Wright and

Schoellhamer 2004, Canuel et al. 2009). Glibert et al. (2014) attributed recent phytoplankton

blooms in Suisun Bay to a drought, during which residence times and nitrification rates increased.

Speciation changes in the dominant forms of nitrogen are considered key factors that contribute to

phytoplankton blooms, particularly seasonal reductions in ammonium that allow uptake of nitrate

that stimulates growth (Dortch 1990, Dugdale et al. 2007). Changes in phytoplankton biomass

and the effects on pelagic organisms have also been of concern. Jassby (2008) described decadal

trends in phytoplankton biomass to understand mechanisms of decline for pelagic fish populations

in the Delta. Although phytoplankon concentrations have been relatively consistent in Suisan

Bay, biomass in the upper Delta has been increasing. Much of these trends were explained by

invasion of benthic grazers in polyhaline areas and changes in the mean flow conditions observed

in the Delta.

Long-term monitoring data are powerful sources of information that can facilitate

descriptions of water quality change in coastal regions. A comprehensive water quality

monitoring program has been in place in the Delta for several decades (Fig. 1, IEP 2013).

Although these data have been used extensively, water quality trends covering the full spatial and

temporal coverage of the monitoring dataset have not been systematically evaluated. Quantitative

descriptions of nutrient dynamics in the Delta are challenging given multiple sources and the

volume of water that is exchanged with natural and anthropogenic processes. An evaluation using

mass-balance models to describe nutrient dynamics in the Delta demonstrated that the majority of ammonium entering the system during the summer is nitrified or assimilated, whereas a considerable percentage of total nitrogen load to the Delta is exported to the estuary (Novick et al. 2015). Seasonal and annual changes in the delivery of water inflows and water exports directly from the system can also obscure trends (Jassby and Cloern 2000, Jassby 2008).

Formal methods for trend analysis are required to describe water quality changes that vary by space and time. As a practical approach for water quality evaluation, trend analysis of ecosystem response indicators often focuses on tracking the change in concentrations or loads of nutrients over many years. Response indicators can vary naturally with changing flow conditions and may also reflect long-term effects of management or policy changes. For example, chl-*a* concentration as a measure of phytoplankton response to nutrient inputs can follow seasonal patterns with cyclical variation in temperature and light changes throughout each year, whereas annual trends can follow long-term variation in nutrient inputs to the system (Cloern 1996, Cloern and Jassby 2010). Similarly, nutrient trends that vary with hydrologic loading also vary as a function of utilization rates by primary producers or decomposition processes (Sakamoto and Tanaka 1989, Schultz and Urban 2008, Harding et al. 2016).

The Weighted Regressions on Time, Discharge, and Season (WRTDS) approach was developed in this context and has been used to characterize decadal trends in running-water systems (Hirsch et al. 2010, Sprague et al. 2011, Medalie et al. 2012, Hirsch and De Cicco 2014, Pellerin et al. 2014, Zhang et al. 2016). The WRTDS method has been adapted for trend analysis in tidal waters, with a focus on chl-*a* trends in Tampa Bay (Beck and Hagy III 2015) and the Patuxent River Estuary (Beck and Murphy 2017). Although the WRTDS method has been effectively applied to describe changes in freshwater systems, use in coastal ecosystems has not

5

been as extensive. Application of WRTDS to describe trends in estuaries could reveal new

insights given the disproportionate effects of physical drivers, such as flow inputs and tidal

exchange, on water quality. The effects of biological drivers may also be more apparent because

hydrological effects can be removed by WRTDS. As such, application of WRTDS models for

trend analysis could facilitate a broader discusion on the need to focus beyond nutrients to

develop integrated plans for water quality management.

The goal of this study was to provide a comprehensive description of nutrient trends in the

Delta region to inform understanding of ecosystem response dynamics and potential causes of

water quality change. This study also supports a general need to more effectively use long-term

monitoring data to inform management priorities for water quality in coastal regions. The specific

objectives were to 1) quantify and interpret trends over four decades at ten stations in the Delta,

including annual, seasonal, and spatial changes in nitrogen analytes and response to flow

variation, and 2) provide detailed descriptions of two case studies in the context of conceptual

relationships modeled with WRTDS. The second objective evaluated two specific water quality

stations to demonstrate complexities with nutrient response to flow, effects of nutrient-related

source controls on ambient conditions, and effects of biological invasion by benthic filter feeders

on primary production. Our general hypothesis was that the results were expected to support

previous descriptions of trends in this well-studied system, but that new insight into spatial and

temporal variation in response endpoints was expected, particuarly in flow-normalized model

predictions.

2   *Materials and Methods*

2.1   Study system

The Delta region drains a 200 thousand km^2 watershed into the SFE, which is the largest

estuary on the Pacific coast of North America. The watershed provides water to over 25 million

people and irrigation for 18 thousand km^2 of agricultural land. Water enters the SFE through the

Sacramento and San Joaquin rivers that have a combined inflow of approximately 28 km^3 per

year, with the Sacramento accounting for 84% of inflow to the Delta. The SFE system includes

the Delta and subembayments of San Francisco Bay (Fig. 1). Water dynamics in the SFE and

Delta are governed by inflows from the watershed, tidal exchange with the Pacific Ocean, and

water withdrawals for municipal and agricultural use (Jassby and Cloern 2000). Seasonally,

inflows from the watershed peak in the spring and early summer from snowmelt, whereas

consumption, withdrawals, and export have steadily increased from 1960 to present, but vary

depending on inter-annual climate effects (Cloern and Jassby 2012). Notable drought periods

have occurred from 1976-1977, 1987-1992, and recently from 2013-2015 (Cloern 2015).

Orthophosphate (PO$_4^{3-}$) and dissolved inorganic nitrogen (DIN) enter the Delta primarily

through the Sacramento and San Joaquin rivers and from municipal WWTP inputs. Annual

nutrient export from the Delta region has been estimated as approximately 30 thousand kg d^{-1} of

total nitrogen (varying with flow, Novick et al. 2015), with 90% of ammonium (NH$_4^+$) originating

solely from the Sacramento Regional WWTP (Jassby 2008). Although nitrogen and phosphorus

inputs are considerable, primary production is relatively low and not nutrient-limited (Jassby et al.

2002, Kimmerer et al. 2012). The resistance of SFE to the negative effects of eutrophication has

historically been attributed to its unique physical and biological characteristics, including strong tidal mixing that limits stratification in the larger estuary (Cloern 1996, Thompson et al. 2008), limits on phytoplankton growth from high turbidity, and filter-feeding by bivalve mollusks in the northern portion (Thompson et al. 2008, Crauder et al. 2016). However, recent water quality trends have suggested that resilience to nutrient inputs is decreasing(Lehman et al. 2005, Cloern et al. 2007, Lehman et al. 2010), which has been attributed to biological invasions (Cohen and Carlton 1998) and departures from the historical flow record (Enright and Culberson 2009, Cloern and Jassby 2012), among other factors acting at global scales (e.g., variation in sea surface temperatures, Cloern et al. 2007).

2.2   Data sources

Nutrient time series of monthly observations from 1976 to 2013 were obtained for ten active sampling stations in the Delta (Fig. 1 and Table 1, IEP 2013). Stations were grouped by location in the study area for comparison: peripheral Delta stations C3 (Sacramento inflow), C10 (San Joaquin inflow), MD10, P8; interior Delta stations D19, D26, D28; and Suisun stations D4, D6, and D7. These stations cover all of the major inflows and outflows to the Delta and were selected for analysis based on the continuity of the period of observation (Jabusch and Gilbreath 2009). Although many other stations are available for the region, the stations were chosen because they are actively maintained by the regional monitoring program and they capture dominant seasonal and annual modes of nitrogen variability characteristic of the region (Jabusch et al. 2016). Time series were complete for all stations except for an approximate ten year gap from 1996-2004 for D19. Data were minimally processed, with the exception of averaging replicates that occurred on the same day. The three nitrogen analytes that were evaluated were

ammonium, nitrite/nitrate, and DIN (as the sum of the former two). Less than 3% of all observations were below the deteciton limit (left-censored), although variation was observed between analytes and location. The ammonium time series had the most censored observations at sites C10 (25.4% of all observations), MD10 (18.1%), D28 (17.8%), D19 (12%), and D7 (7.9%).

WRTDS models require flow data paired with nutrient data. At the peripheral and interior stations, daily flow estimates were matched with the corresponding sample dates for the nutrient data. Daily flow estimates were obtained from the Dayflow software program (IEP 2016). The Sacramento daily flow time series was used to account for flow effects at C3, D19, D26, D28, and MD10, and the San Joaquin time series was used for C10 and P8 based on station proximity to each inflow. Given the complexity of inflows and connectivity of the system, only the inflow estimates from the Sacramento and San Joaquin rivers were used as measures of freshwater influence at each station. Initial analyses indicated that model fit was not significantly improved with flow estimates from locations closer to each station, nor was model fit improved using lagged times series. Salinity was used as a proxy for flow at sites D4, D6, and D7 where tidal influences were much stronger. Salinity has been used as a tracer of freshwater influence for the application of WRTDS models in tidal waters (Beck and Hagy III 2015). Models were evaluated using salinity at the interior and peripheral stations but performance was reduced relative to models that used daily flow estimates.

2.3 Analysis method and application

A total of thirty WRTDS models were created, one for each nitrogen analyte at each station. The functional form of WRTDS is a simple regression (Hirsch et al. 2010) that models the log-transformed response variable as a function of time, flow, and season:

9

$$\ln{(N)} = \beta_0 + \beta_1 t + \beta_2 \ln{(Q)} + \beta_3 \sin{(2\pi t)} + \beta_4 \cos{(2\pi t)} \tag{1}$$

176 where N is one of three nitrogen analytes, time t is a continuous variable as decimal time to

177 capture the annual (β_1) or seasonal trend (β_3, β_4), and Q is the flow variable (either flow or

178 salinity depending on station). Generally, the WRTDS model is a moving window regression that

179 fits unique parameters (i.e., $\beta_0, \ldots, \beta_4$) at each observation point in the time series (n ranging

180 from 433 at D19 to 571 at C3). Rather than fitting a global model to the entire time series, one

181 regression is fit to every observation. Observations within a window for each regression are

182 weighted relative to annual, seasonal, and flow distances from the observation at the center of the

183 window. Observations with distances farther from the center (i.e., greater time and different flow

184 values from the center) have less weight during parameter estimation for each regression. This

185 approach allows for a type of smoothing where the observed fit is specific to the data

186 characteristics within windows. Models applied herein were based on a tidal adaptation of the

187 original method that can use either flow or salinity estimates as nutrient predictors (Beck and

188 Hagy III 2015). All models were fit to describe the conditional mean response using a weighted

189 Tobit model for left-censored data below the detection limit (Tobin 1958). Model predictions

190 were evaluated as monthly values or as annual values that averaged monthly results within each

191 water year (October to September). All analyses used the WRTDStidal package for the R

192 statistical programming language (Beck 2017, RDCT (R Development Core Team) 2017). The

193 default model fitting procedures were used that set half-window widths as six months for seasonal

194 weights, ten years for annual weights, and half the range of salinity or flow in the input data for Q

195 weights.

A hallmark of the WRTDS approach is the description of flow-normalized trends that are independent of variation from freshwater inflows (Hirsch et al. 2010). Flow-normalized trends for each analyte at each station were used to describe long-term changes in different annual and seasonal periods. Flow-normalization predictions for each month of each year were based on the average of predictions for flow values that occur in the same month across all years, weighted within each specific month and year for every observation. Flow-normalized trends in each analyte were summarized as both medians and percent changes from the beginning to end of annual groupings from 1976-1995 and 1996-2013, and seasonal groupings of March-April-May (spring), June-July-August (summer), September-October-November (fall), and December-January-February (winter) within each annual grouping. Annual groupings were chosen as approximate twenty year midpoints in the time series and seasonal groupings were chosen to evaluate inter-annual changes while keeping season constant.

Trends in each annual and seasonal grouping were based on seasonal Kendall tests of the flow-normalized predictions. This test is a modification of the non-parametric Kendall test that accounts for variation across seasons in the response variable (Hirsch et al. 1982, Millard 2013). Results from the test can be used to evaluate the direction, magnitude, and significance of a monotonic change within the period of observation. The estimated rate of change per year is also returned as the Theil-Sen slope and was interpreted as the percent change per year when divided by the median value of the response variable in the period of observation (Jassby 2008). Trends in annual groupings were based on all monthly observations within relevant years, whereas seasonal groupings were based only on the relevant months across years. Seasonal Kendall tests were also used to describe trends in the observed data. These trends were compared with those based on the flow-normalized trends to evaluate potential differences in conclusions caused by flow effects.

11

2.4 Selected examples

Two stations were chosen to demonstrate use of WRTDS to develop a more comprehensive description of decadal trends in the Delta. The selected case studies focused on 1) effects of wastewater treatment upgrades upstream of P8, and 2) effects of biological invasion on nutrient dynamics in Suisun Bay using observations from D7. Each case study is built around hypotheses that results from WRTDS models were expected to support, both as a general description and for additional testing with alternative methods.

2.4.1 Effects of wastewater treatment

Significant efforts have been made in recent years to reduce nitrogen loading from regional WWTPs given the disproportionate contribution of nutrients relative to other sources (Cornwell et al. 2014, Novick et al. 2015). Several WWTPs in the Delta have recently been or are planned to be upgraded to include tertiary filtration and nitrification to convert biologically available ammonium to nitrate. The City of Stockton WWTP was upgraded in 2006 and is immediately upstream of station P8 (Jabusch et al. 2016), which provides a valuable opportunity to assess how nutrient or nutrient-related source controls and water management actions have changed ambient concentrations downstream. An increase and decrease of nutrient concentrations at P8 centered around 2006 is expected as a result of upstream WWTP upgrades, and water quality should exhibit 1) a shift in the ratio of the components of DIN from the WWTP before/after upgrade, and 2) a flow-normalized annual trend at P8 to show a change concurrent with WWTP upgrades.

2.4.2 Effects of biological invasions

Invasion of the upper SFE by the Asian clam *Potamocorbula amurensis* in 1986 caused severe changes in phytoplankton abundance and species composition. Reduction in phytoplankton

biomass has altered trophic networks in the upper SFE and is considered an important mechanism in the decline of the protected delta smelt (*Hypomesus transpacificus*) and other important fisheries (Feyrer et al. 2003, Mac Nally et al. 2010). Changes in the physical environment have also occurred, particularly increased water clarity from a reduction of particle transport and erodible sediment supply (Jassby 2008, Schoellhamer 2011, Cloern and Jassby 2012), although decreases in phytoplankton by clam biofiltration may have also increased clarity (Mac Nally et al. 2010). The clams are halophilic such that drought years are correlated with an increase in biomass and further upstream invasion of the species (Parchaso and Thompson 2002, Cloern and Jassby 2012). We hypothesized that results from WRTDS models would show 1) a decline in annual, flow-normalized chlorophyll concentrations over time coincident with an increase in abundance of invaders, and 2) variation in the chlorophyll/clam relationship through indirect or direct controls of flow. Although the relationship between phytoplankton and clams have been well described in SFE (Kimmerer and Thompson 2014), we use WRTDS to develop additional evidence that an increase in DIN was facilitated in part by clam invasion and the relationship of phytoplankton with clam abundance was mediated by flow and climatic variation in recent years.

3   Results

3.1   Observed and modelled Data

The observed time series for the ten Delta - Suisun Bay stations had substantial variation in scale among the nitrogen analytes and differences in apparent seasonal trends (Fig. 2). DIN for most stations was dominated by nitrite/nitrate, whereas ammonium was a smaller percentage of the total. However, C3 had a majority of DIN composed of ammonium and other stations (e.g., P8, D26) had higher concentrations of ammonium during winter months when assimilation rates

are lower (Novick et al. 2015). By location, observed concentrations of DIN for the entire time series were higher on average for the peripheral stations (C3, C10, MD10, P8; mean $\pm$ s.e.: 1.04 ± 0.03 mg L^{-1}) and similar for the interior (D19, D26, D28, 0.43 ± 0.01) and Suisun Bay stations (D4, D6, D7, 0.44 ± 0.01). Average concentrations were highest at P8 (1.63 ± 0.05 mg L^{-1}) and lowest at C3 (0.4 ± 0.01) for DIN, highest at P8 (0.28 ± 0.02) and lowest at D28 (0.05 ± 0.003) for ammonium, and highest at C10 (1.4 ± 0.04) and lowest at C3 (0.15 ± 0.004) for nitrite/nitrate. Mean observed concentrations were also higher later in the time series for all analytes. For example, average DIN across all stations was 0.61 ± 0.01 mg L^{-1} for 1976-1995, compared to 0.7 ± 0.01 for 1996-2013. Seasonal changes across all years showed that nitrogen concentrations were generally lower in the summer and higher in the winter, although observed patterns were inconsistent between sites. For example, site MD10 had distinct seasonal spikes for elevated DIN in the winter, whereas other stations had less prominent seasonal maxima (e.g., C3, D7, Fig. 2).

Long-term trends between stations for the different nitrogen analytes were apparent from the modelled results (Fig. 3). Although each station varied in the overall concentrations, patterns within the three Deltra regions (peripheral, interior, and Suisun) were observed. Concentrations for all nitrogen analytes were highest in the peripheral stations. Ammonium concentrations at P8 and C3 were highest and showed a consistent increase over time, followed by a reduction beginning in the early 2000s, whereas ammonium concentrations at C10 and MD10 were low and gradually decreasing throughout the period of record. By contrast, DIN and nitrite/nitrate concentrations at the peripheral stations showed increases at P8 and C10 followed by a decline in the early 2000s, whereas concentrations at C3 and MD10 were lower and did not show any noticeable trends. Trends in the interior stations showed a gradual increase in ammonium

14

followed by a gradual decrease beginning in the early 1990s, particularly for D26. Trends in DIN and nitrite/nitrate for the interior stations showed a reduction early in the time series, followed by a slight increase beginning in the mid-1980s, and finally a reduction beginning in the late 1990s. These trends were similar for the Suisun stations, although the reduction in the late 1990s did not occur. By contrast, ammonium concentrations were low in Suisun but a gradual increase over the period of record was observed.

3.2   Trend tests

Estimated trends from Seasonal Kendall tests on the raw time series varied considerably between sites and analytes (Fig. 4). Significant trends were observed from 1976-1995 for eight of ten sites for DIN (seven increasing, one decreasing), eight sites for ammonium (six increasing, two decreasing), and six sites for nitrite/nitrate (five increasing, one decreasing). Decreasing trends were more common for the observed data from 1996-2013. Eight sites had significant trends for DIN (four increasing, four decreasing), seven sites for ammonium (five increasing, two decreasing), and eight sites for nitrite/nitrate (four increasing, four decreasing). P8 had a relatively large decrease in ammonium (-8.3% change per year) for the second annual period compared to all other sites. Trends by season were similar such that increases were generally observed in all seasons from 1976-1995 (Fig. S1) and decreases were observed for 1996-2013 (Fig. S2). Trends for the seasonal comparisons were noisier and significant changes were less common compared to the annual comparisons.

A comparison of flow-normalized results from WRTDS relative to observed data identified changes in the magnitude, significance, and direction of trends. For all sixty trend comparisons in Fig. 4 (flow-normalized values in Table 2) regardless of site, nitrogen analyte, and

15

time period (annual or seasonal aggregations), thirteen comparisons had trends that were

insignificant ($p > 0.05$) with the observed data but significant with flow-normalized results,

whereas only one trend changed to insignificant. This suggests that time series that include flow

effects had sufficient noise to obscure or prevent identification of an actual trend of a water

quality parameter. Further, changes in the magnitude of the estimated percent change per year

were also apparent for the flow-normalized trends, such that fourteen comparisons showed an

increase in magnitude (more negative or more positive) and twenty five had a decrease (less

positive or less negative) compared to observed trends. Eleven comparisons showed a trend

reversal from positive to negative estimated change, nine sites went from no change to negative

estimated change, and one site went from no change to a positive trend for the flow-normalized

results. Differences by season in the observed relative to flow-normalized trends from WRTDS

were also apparent (Figs. S1 and S2 and Tables S1 and S2). The most notable changes were an

overall decrease in the estimated trend for most sites in the summer and fall seasons for

1996-2013, including an increase in the number of statistically significant trends.

3.3 Selected examples

3.3.1 *Effects of wastewater treatment*

Effluent measured from 2003 to 2009 from the Stockton WWTP had similar DIN

concentrations before and after upgrades, whereas ammonium concentrations were greatly

reduced (Fig. 5). Ammonium and nitrate concentrations were comparable prior to 2006, whereas

nitrate was a majority of total nitrogen after the upgrade, with much smaller percentages from

ammonium and nitrite. As expected, flow-normalized nitrogen trends at P8 shifted in response to

upstream WWTP upgrades (Fig. 6a), with ammonium showing an increase from 1976 followed

16

by a large reduction in the 2000s. Nitrite/nitrate concentrations at P8 also showed a similar but less dramatic decrease despite an increase in the WWTP effluent concentrations following the upgrade (Fig. 5). Percent changes from seasonal Kendall tests on flow-normalized results (Table 3) showed that both nitrogen species increased prior to WWTP upgrades (2% per year for nitrite/nitrate, 2.8% for ammonium), followed by decreases after upgrades (-1.9% for nitrite/nitrate, -16.6% for ammonium). Seasonally, increases prior to upgrades were highest in the summer for nitrite/nitrate (2.4%) and in the fall for ammonium (4.9%). Similarly, seasonal reductions post-upgrade were largest in the summer for nitrite/nitrate (-4.3%) and largest for ammonium in the winter (-26.7%).

Nitrogen concentrations varied with flow, although relationships depended on season and year. Relationships of nitrite/nitrate with flow described by WRTDS showed flushing or dilution at higher flow (Fig. 6b). Seasonal variation was even more apparent for ammonium, although both nitrite/nitrate and ammonium typically had the highest concentrations at low flow in the winter (January). Additionally, strength of the flow/nutrient relationship changed between years. Nitrite/nitrate typically had the strongest relationship with flow later in the time series (i.e., larger negative slope), whereas ammonium had the strongest relationship with flow around 2000 in January.

3.3.2 *Effects of biological invasions*

Invasion in the 1980s showed a clear reduction of *Corbicula fluminea* and increase of *P. amurensis* (Fig. 7a), where biomass of the latter was negatively associated with flow from the Sacramento river (Fig. 7b). The increase in clam abundance was associated with a notable decrease in annually-averaged chl-*a* from WRTDS results (Fig. 7c), as expected if WRTDS is adequately capturing flow variation and identifying the well-established phytoplankton decrease

17

beginning in the 1980s. A seasonal shift in the flow-normalized results was also observed such that chl-*a* concentrations were generally highest in July/August prior to invasion, whereas a spring maximum in April was more common in recent years (Fig. 7f). An increase in annually-averaged silicon dioxide (Fig. 7d) was coincident with the chl-*a* decrease, with the largest increases occuring in August (Fig. 7g). Further, DIN trends were similar to silicon-dioxide in both annual and seasonal changes (i.e., Figures 7e and 7h compared to 7d and 7g), such that an increase in both nutrients earlier in the time series corresponded with the decrease in chl-*a*.

The relationship of chl-*a* with clam biomass was significant (Fig. 7i), with lower chl-*a* associated with higher biomass. However, the effect of flow on both clams and phytoplankton as a top-down or bottom-up control changed throughout the time series. The chl-*a*/flow relationship showed that increasing flow (decreasing salinity) was associated with a slight increase in chl-*a* followed by a decrease early in the time series (Fig. 7j), whereas overall chl-*a* was lower but a positive association with flow (negative with salinity) was observed later in the time series. Following clam invasion, chl-*a* concentrations were reduced by grazing but showed a positive and monotonic relationship with increasing flow. The increase in clam abundance was concurrent with decline in chl-*a* concentration, although variation in abundance between years was also observed. Clam abundance was reduced during high flow years in the late 1990s, 2006, and 2011 (7a). In the same years, WRTDS predictions for chl-*a* were higher than the flow-normalized component (Fig. 7c), which further suggests a link between increased flow and phytoplankton production.

4   *Discussion*

Water quality conditions in the Delta are dynamic and not easily characterized from observed time series. Annual aggregations of WRTDS modelled results and application of formal

18

trend analyses provided insight into the spatial and temporal variation of nitrogen analytes in three distinct regions of the Delta that is not possible with raw observations. A general conclusion is that nitrogen concentrations have decreased overall throughout the approximate forty years of observation. These results are confirmed visually from WRTDS (Fig. 3) and through significant results from trend tests (Fig. 4, Table 2). Although the overall trends suggest a system-wide reduction, considerable differences by location and analyte were characterized by the analysis and are important independent of overall trends. Nutrient concentrations were highest at the peripheral stations (C3, MD10, P8, and C10) that monitor inflows from the Sacramento, San Joaquin, Cosumnes, and Mokelumne rivers. The highest concentrations among all nitrogen analytes, ammonium in particular, were observed at P8 as a direct consquence of WWTP inputs upstream. Elevated ammonium concentrations were also observed at C3 as a measure of upstream contributions from the Sacramento Regional County Sanitation District. By contrast, nitrite/nitrate concentrations were highest at C10 as a measure of contributions from the San Joaquin River to the south that drains a predominantly agricultural watershed. Although the Sacramento River drains a much larger area, the dominant ammonium signal as compared to nitrite/nitrate at C3 underscores the importance of WWTP control for water quality issues downstream.

Differing magnitudes of nitrogen analytes between stations as a function of source type can have an effect on the relationship between flow and nutrients. Both Hirsch et al. (2010) and Beck et al. (2015) used WRTDS results to demonstrate variation between flow and nutrient dynamics depending on pollutant sources. In particular, a chemodynamic response of nutrients with flow variation is common if nutrients originate primarily from the watershed through diffuse sources (Thompson et al. 2011, Wan et al. 2017). Increased flow may induce a change in nutrient

concentrations, such that reduction may occur with flushing or an increase may occur through mobilization. By contrast, nutrient loads are relatively chemostatic or invariant with changes in flow if point-sources are the dominant contributor. These relationships are modelled particularly well with WRTDS, which can provide a means of hypothesizing unknown sources or verifying trends in response to management actions. As noted above, C10 at the inflow of the San Joaquin River is dominated by nitrite/nitrate consistent with diffuse, agricultural inputs from the watershed. A logical expectation is that trends from observed data may vary considerably from trends with modelled results that are flow-normalized. Accordingly, trend analysis of nitrate/nitrate by year and season showed that percent changes at C10 were typically underestimated with the observed data during the recent period from 1996-2013 (Tables 2 and S2). This is consistant with an expected effect of flow on raw time series, particularly for chemodynamic behavior at locations that drain highly developed watersheds (Wan et al. 2017).

Our results demonstrated the potential to interpret different trends if flow effects are not considered, where the difference could vary from a simple change in the magnitude and significance of a trend, to more problematic changes where the flow-normalized trend could demonstrate a complete reversal relative to the observed (e.g., DIN trends for all Suisun stations from 1996-2013, Fig. 4). Differences in apparent trends underscore the importance of considering flow effects in the interpretation of environmental changes, particularly if trend evaluation is used to assess the effects of nutrients on ecosystem health or the effectiveness of past nutrient management actions. An alternative evaluation of flow in the Delta demonstrated that flow contributions from different sources vary considerably over time at each station (Novick et al. 2015). For example, flow at MD10 represents a changing percentage by season of inputs from the Sacramento, San Joaquin, Cosumnes, Mokelumne rivers, and agricultural returns. For simplicity,

20

water quality observations in our analyses were matched with large-scale drivers of flow into the Delta where most sites were matched to Sacramento or San Joaquin daily flow estimates. Given that substantial differences with flow-normalized results were apparent from relatively coarse estimates of flow contributions, more precise differences could be obtained by considering the influence of multiple flow components at each location. Output from the Dayflow software program (IEP 2016) provides a complete mass balance of flow in the Delta that could be used to develop a more comprehensive description.

Long-term trends in nutrient and phytoplankton concentrations in Suisun Bay have also been the focus of intense study for many years (Cloern et al. 1983, Lehman 1992, Dugdale et al. 2007, Jassby 2008, Glibert et al. 2014). Although nitrite/nitrate concentrations generally exceed ammonium about five-fold at the Suisun Bay stations, changes in ammonium concentration below 0.072 mg L^{-1} (4 μmol L^{-1}) is a concern given the affect on the uptake of nitrate by phytoplankton (Dugdale et al. 2007). Energetic costs of ammonium for phytoplankton growth are lower than nitrate such that the former tends to stimulate growth in most cases. Although phytoplankton communities in SFE generally utilize ammonium when growth conditions are favorable, seasonal variation in the dominant forms has contributed to occurrence of bloom events in recent years. In particular, reduction of ammonium in the spring in Suisun Bay below thresholds of 4 μmol L^{-1} has contributed to uptake of nitrate that stimulates bloom development. Our results demonstrated an overall increase in ammonium from the late 1970s to 2000, with initial flow-normalized values of annual averages estimated as approximately 0.05 mg L^{-1} for the Suisun stations in 1976 to a maximum ranging from 0.08 mg L^{-1} (station D4) to above 0.1 mg L^{-1} (D6) in 2000 (Fig. 3). Trends from 1996-2005 evaluated in (Jassby 2008) showed a similar increase in ammonium. However, a reversal of trends in in recent years may also be occuring in

21

Suisun Bay, as model estimates suggest either relatively constant concetratrations or even a decrease at some stations beginnign around 2000 (e.g., D6, D7, Fig. 4). Combined with the shift towards a dominant spring peak in chloropyll growth (Fig. 7f), changing nitrogen ratios continue to be a concern for the management of production in the upper SFE.

4.1   Interpretation of case studies

Seasonal timings of water quality improvements and the link to flow changes are difficult to characterize from the observed time series. WRTDS models were used to characterize these changes at P8 and to develop additional hypotheses of factors that influence nutrient concentrations. A general conclusion is that ammonium reductions were concurrent with WWTP upgrades, but the reduction was most apparent at low-flow in January. Estimated ammonium concentrations in July were low for all flow levels, which suggests either nitrogen inputs were low in the summer or nitrogen was available but uptake by primary consumers and bacterial processing were high. Seasonal patterns in the relationship between flow and nitrite/nitrate were not as dramatic as compared to ammonium, and in particular, low-flow events in July were associated with higher concentrations. This could suggest that ammonium concentrations at P8 are driving phytoplankton production at low flow during warmer months, and not nitrite/nitrate given the higher estimated concentrations in July at low flow. As such, these simple observations provide quantitative support of cause and effect mechanisms of nutrient impacts on potentially adverse environmental conditions as they relate to nutrient-related source controls upstream. Additional research could investigate these hypotheses to better describe mechanisms of change as a basis for more informed management.

The results for Suisun Bay provide additional descriptions of change in production as it

22

relates to flow, grazing, and nitrogen ratios. In general, clam biomass was associated with a decrease in chl-*a* concentration, as shown by others (Alpine and Cloern 1992, Thompson et al. 2008). Our results also suggested that diatoms were the dominant genera early in the time series, particularly in late summer, whereas the spring peak observed in later years represents a shift to an earlier seasonal maxima. This supports past research that showed a decrease in silica uptake by diatoms following invasion (Cloern 1996, Kimmerer 2005). Anontrivial portion of the DIN increase could be related to the decrease in a major 'sink', i.e., decreased DIN uptake by phytoplankton due to top down grazing pressure from *P. amurensis*. Flow effects on phytoplankton production have also changed over time. In the absence of benthic grazing prior to invasion, chl-*a* production was limited at low flow as less nutrients were exported from the Delta, stimulated as flow increases, and reduced at high flow as either nutrients or phytoplankton biomass are exported to the estuary (Fig. 7j). Recent years have shown a decrease in overall chlorophyll, with particularly low concentrations at low flow (high salinity). As such, chl-*a* production in early years is directly related to flow, whereas the relationship with flow in later years is indirect as increased flow reduces clam abundance and releases phytoplankton from benthic grazing pressure. These relationships have been suggested by others (Cloern et al. 1983, Alpine and Cloern 1992, Parchaso and Thompson 2002, Jassby 2008), although the precise mechanism demonstrated by WRTDS provides a quantitative description of factors that drive water quality in the Delta.

4.2 Conclusions

As demonstrated by both case studies and the overall trends across all stations, water quality dynamics in the Delta are complex and driven by multiple factors that change through

space and time. WRTDS models can facilitate descriptions of change by focusing on high-level

forcing factors that explicitly account for annual, seasonal, and flow effects on trend

interpretations. We have demonstrated the potential for imprecise or inaccurate conclusions of

trend tests that focus solely on observed data and emphasize that flow-normalized trends have

more power to quantify change. The results from WRTDS are also consistent with described

trends of nutrient loads from point sources (e.g., Sacramento WWTP increases (Jassby 2008) and

exports to Suisun Bay (Novick and Senn 2014)) demonstrating that these changes are not

unexpected. Consequently, we are not detracting from the potential implications of such

increases. The important conclusion is that the physical/hydrological and biogeochemical factors

that influence nutrient cycling and ambient concentrations in the Bay-Delta, and changes to those

factors, are substantial enough that they can be comparable in magnitude to anthropogenic load

increases or comparable to the effects of management actions to decrease nutrient levels.

Therefore, methods that adjust for the effects of these factors are critical when studying long-term

records to assess the impacts or effectiveness of load increases or management actions,

respectively.

Combined with additional data, our results can support hypotheses that lead to a more

comprehensive understanding of ecosystem dynamics. Additional factors to consider include the

effects of large-scale climatic patterns, more detailed hydrologic descriptions, and additional

ecological components that affect trophic interactions. For example, a more rigorous matching of

flow time series with water quality observations at each station that considers varying source

contributions over time could provide a more robust description of flow effects. Alternative

methods could also be used to address a wider range of questions, particularly those with more

generic structural forms that can explicitly include additional variables (e.g., generalized additive

24

models, Beck and Murphy (2017)). Overall, quantitative interpretations of multiple factors can

provide a basis for identifying links between nutrient loads and adverse effects on ecosystem

conditions, including the identification of thresholds for the protection and restoration of water

quality.

Acknowledgments

References

Alpine AE, Cloern JE. 1988. Phytoplankton growth rates in a light-limited environment, San
    Francisco Bay. Marine Ecology Progress Series, 44(2):167–173.

Alpine AE, Cloern JE. 1992. Trophic interactions and direct physical effects control
    phytoplankton biomass and production in an estuary. Limnology and Oceanography,
    37(5):946–955.

Beck MW. 2017. WRTDStidal: Weighted Regression for Water Quality Evaluation in Tidal
    Waters. R package version 1.1.0.

Beck MW, Hagy III JD. 2015. Adaptation of a weighted regression approach to evaluate water
    quality trends in an estuary. Environmental Modelling and Assessment, 20(6):637–655.

Beck MW, Hagy III JD, Murrell MC. 2015. Improving estimates of ecosystem metabolism by
    reducing effects of tidal advection on dissolved oxygen time series. Limnology and
    Oceanography: Methods, 13(12):731–745.

Beck MW, Murphy RR. 2017. Numerical and qualitative contrasts of two statistical models for
    water quality change in tidal waters. Journal of the American Water Resources Association,
    53(1):197–219.

Canuel EA, Lerberg EJ, Dickhut RM, Kuehl SA, Bianchi TS, Wakeham SG. 2009. Changes in sediment and organic carbon accumulation in a highly-disturbed ecosystem: The Sacramento-San Joaquin River Delta (California, USA). Marine Pollution Bulletin, 59(4-7):154–163.

Cloern JE. 1996. Phytoplankton bloom dynamics in coastal ecosystems: A review with some general lessons from sustained investigation of San Francisco Bay, California. Review of Geophysics, 34(2):127–168.

Cloern JE. 2001. Our evolving conceptual model of the coastal eutrophication problem. Marine Ecology Progress Series, 210:223–253.

Cloern JE. 2015. Life on the edge: California's estuaries. In: Mooney H, Zavaleta E, editors, Ecosystems of California: A Source Book, pages 359–387. University of California Press, California.

Cloern JE, Alpine AE, Cole BE, Wong RLJ, Arthur JF, Ball MD. 1983. River discharge controls phytoplankton dynamics in the northern San Francisco Bay estuary. Estuarine, Coastal and Shelf Science, 16(4):415–426.

Cloern JE, Jassby AD. 2010. Patterns and scales of phytoplankton variability in estuarine-coastal ecosystems. Estuaries and Coasts, 33(2):230–241.

Cloern JE, Jassby AD. 2012. Drivers of change in estuarine-coastal ecosystems: Discoveries from four decades of study in San Francisco Bay. Reviews of Geophysics, 50(4):1–33.

Cloern JE, Jassby AD, Thompson JK, Hieb KA. 2007. A cold phase of the East Pacific triggers new phytoplankton blooms in San Francisco Bay. Proceedings of the National Academy of Sciences of the United States of America, 104(47):18561–18565.

Cloern JE, Schraga TS, Lopez CB, Knowles N, Labiosa RG, Dugdale R. 2005. Climate anomalies generate an exceptional dinoflagellate bloom in San Francisco Bay. Geophysical Research Letters, 32(14):L14608.

Cohen AN, Carlton JT. 1998. Accelerating invasion rate in a highly invaded estuary. Science, 279(5350):555–558.

Cole BE, Cloern JE. 1984. Significance of biomass and light availability to phytoplankton productivity in San Francisco Bay. Marine Ecology Progress Series, 17(1):15–24.

Cornwell JC, Glibert PM, Owens MS. 2014. Nutrient fluxes from sediments in the San Francisco Bay Delta. Estuaries and Coasts, 37(5):1120–1133.

Crauder JS, Thompson JK, Parchaso F, Anduaga RI, Pearson SA, Gehrts K, Fuller H, Wells E. 2016. Bivalve effects on the food web supporting delta smelt - a long-term study of bivalve recruitment, biomass, and grazing rate patterns with varying freshwater outflow. Technical Report Open-File Report 2016-1005, US Geological Survey, Reston, Virginia.

573 Dortch W. 1990. The interaction between ammonium and nitrate uptake in phytoplankton.
574   Marine Ecology Progress Series, 61(1/2):183–201.

575 Dugdale RC, Wilkerson FP, Hogue VE, Marchi A. 2007. The role of ammonium and nitrate in
576   spring bloom development in San Francisco Bay. Estuarine, Coastal, and Shelf Science,
577   73:17–29.

578 Enright C, Culberson SD. 2009. Salinity trends, variability, and control in the northern reach of
579   the San Francisco Estuary. San Francisco Estuary and Watershed Science, 7(2):1–28.

580 Feyrer F, Herbold B, Matern SA, Moyle PB. 2003. Dietary shifts in a stressed fish assemblage:
581   Consequences of a bivalve invasion in the San Francisco Estuary. Environmental Biology of
582   Fishes, 67(3):277–288.

583 Glibert PM, Dugdale RC, Wilkerson F, Parker AE, Alexander J, Antell E, Blaser S, Johnson A,
584   Lee J, Lee T, Murasko S, Strong S. 2014. Major - but rare - spring blooms in san francisco bay
585   delta, california, a result of long-term drought, increased residence time, and altered nutrient
586   loads and forms. Journal fo Experimental Marine Biology and Ecology, 460:8–18.

587 Harding LW, Gallegos CL, Perry ES, Miller WD, Adolf JE, Mallonee ME, Paerl HW. 2016.
588   Long-term trends of nutrients and phytoplankton in Chesapeake Bay. Estuaries and Coasts,
589   39:664–681.

590 Hirsch RM, De Cicco L. 2014. User guide to Exploration and Graphics for RivEr Trends
591   (EGRET) and dataRetrieval: R packages for hydrologic data. Technical Report Techniques and
592   Methods book 4, ch. A10, US Geological Survey, Reston, Virginia.
593   http://pubs.usgs.gov/tm/04/a10/.

594 Hirsch RM, Moyer DL, Archfield SA. 2010. Weighted regressions on time, discharge, and season
595   (WRTDS), with an application to Chesapeake Bay river inputs. Journal of the American Water
596   Resources Association, 46(5):857–880.

597 Hirsch RM, Slack JR, Smith RA. 1982. Techniques of trend analysis for monthly water quality
598   data. Water Resources Research, 18:107–121.

599 IEP. 2013. IEP Bay-Delta Monitoring and Analysis Section, Discrete Water Quality Metadata.
600   http://water.ca.gov/bdma/meta/discrete.cfm.

601 IEP. 2016. Dayflow: An estimate of daily average Delta outflow. Interagency Ecological Program
602   for the San Francisco Estuary. http://www.water.ca.gov/dayflow/.

603 Jabusch T, Bresnahan P, Trowbridge P, Novick E, Wong A, Salomon M, Senn D. 2016. Summary
604   and evaluation of Delta subregions for nutrient monitoring and assessment. Technical report,
605   San Francisco Estuary Institute, Richmond, CA.

606 Jabusch T, Gilbreath AN. 2009. Summary of current water quality monitoring programs in the
607   Delta. Technical report, San Francisco Estuary Institute, Richmond, CA.

Jassby AD. 2008. Phytoplankton in the Upper San Francisco Estuary: Recent biomass trends, their causes, and their trophic significance. San Francisco Estuary and Watershed Science, 6(1):1–24.

Jassby AD, Cloern JE. 2000. Organic matter sources and rehabilitations of the Sacramento-San Joaquin Delta (California, USA). Aquatic Conservation: Marine and Freshwater Ecosystems, 10:323–352.

Jassby AD, Cloern JE, Cole BE. 2002. Annual primary production: Patterns and mechanisms of change in a nutrient-rich tidal ecosystem. Limnology and Oceanography, 47(3):698–712.

Kimmerer W. 2005. Long-term changes in apparent uptake of silica in the San Francisco Estuary. Limnology and Oceanography, 50(3):793–798.

Kimmerer WJ, Parker AE, Lidstrom UE, Carpenter EJ. 2012. Short-term and interannual variability in primary production in the low-salinity zone of the San Francisco Estuary. Estuaries and Coasts, 35:913–929.

Kimmerer WJ, Thompson JK. 2014. Phytoplankton growth balanced by clam and zooplankton grazing and net transport into the low-salinity zone of the San Francisco Estuary. Estuaries and Coasts, 37:1202–1218.

Lehman PW. 1992. Environmental factors associated with long-term changes in chlorophyll concentration in the Sacramento-San Joaquin Delta and Suisun Bay, California. Estuaries, 15(3):335–348.

Lehman PW. 2000. The influence of climate on phytoplankton community biomass in San Francisco Bay Estuary. Limnology and Oceanography, 45(3):580–590.

Lehman PW, Boyer G, Hall C, Waller S, Gehrts K. 2005. Distribution and toxicity of a new colonial *Microcystis aeruginosa* bloom in the San Francisco Bay Estuary, California. Hydrobiologia, 541:87–99.

Lehman PW, Teh SJ, Boyer GL, Nobriga ML, Bass E, Hogle C. 2010. Initial impacts of *Microcystis aeruginosa* blooms on the aquatic food web in the San Francisco Estuary. Hydrobiologia, 637(1):229–248.

Mac Nally R, Thompson JR, Kimmerer WJ, Feyrer F, Newman KB, Sih A, Bennett WA, Brown L, Fleishman E, Culberson SD, Castillo G. 2010. Analysis of pelagic species decline in the upper San Francisco Estuary using multivariate autoregressive modeling (MAR). Ecological Applications, 20(5):1417–1430.

Medalie L, Hirsch RM, Archfield SA. 2012. Use of flow-normalization to evaluate nutrient concentration and flux changes in Lake Champlain tributaries, 1990-2009. Journal of Great Lakes Research, 38(SI):58–67.

Millard SP. 2013. EnvStats: An R Package for Environmental Statistics. Springer, New York.

Nichols FH. 1985. Increased benthic grazing: An alternative explanation for low phytoplankton biomass in northern San Francisco Bay during the 1976-1977 drought. Estuarine, Coastal and Shelf Science, 21(3):379–388.

Novick E, Holleman R, Jabusch T, Sun J, Trowbridge P, Senn D, Guerin M, Kendall C, Young M, Peek S. 2015. Characterizing and quantifying nutrient sources, sinks and transformations in the Delta: synthesis, modeling, and recommendations for monitoring. Technical Report Contribution Number 785, San Francisco Estuary Institute, Richmond, CA.

Novick E, Senn D. 2014. External nutrient loads to San Francisco Bay. Technical Report Contribution Number 704, San Francisco Estuary Institute, Richmond, CA.

Parchaso F, Thompson JK. 2002. Influence of hydrologic processes on reproduction of the introduced bivalve *Potamocorbula amurensis* in northern San Francisco Bay, California. Pacific Science, 56(3):329–345.

Pellerin BA, Bergamaschi BA, Gilliom RJ, Crawford CG, Saraceno JF, Frederick CP, Downing BD, Murphy JC. 2014. Mississippi River nitrate loads from high frequency sensor measurements and regression-based load estimation. Environmental Science and Technology, 48:12612–12619.

RDCT (R Development Core Team). 2017. R: A language and environment for statistical computing, v3.3.2. R Foundation for Statistical Computing, Vienna, Austria. http://www.R-project.org.

Sakamoto M, Tanaka T. 1989. Phosphorus dynamics associated with phytoplankton blooms in eutrophic Mikawa Bay, Japan. Marine Biology, 101(2):265–271.

Schoellhamer DH. 2011. Sudden clearing of estuarine waters upon crossing the threshold from transport to supply regulation of sediment transport as an erodible sediment pool is depleted: San francisco bay, 1999. Estuaries and Coasts, 34:885–899.

Schultz P, Urban NR. 2008. Effects of bacterial dynamics on organic matter decomposition and nutrient release from sediments: A modeling study. Ecological Modelling, 210(1-2):1–14.

Shellenbarger GG, Schoellhamer DH, Morgan TL, Takekawa JY, Athearn ND, Henderson KD. 2008. Dissolved oxygen in Guadalupe Slough and Pond A3W, South San Francisco Bay, California, August and September 2007. Technical Report Open-File Report 2008-1097, US Geological Survey, Reston, Virginia.

Sprague LA, Hirsch RM, Aulenbach BT. 2011. Nitrate in the Mississippi River and its tributaries, 1980 to 2008: Are we making progress? Environmental Science and Technology, 45(17):7209–7216.

Sutula M, Kudela R, III JDH, Jr. LWH, Senn D, Cloern JE, Bricker S, Berg GM, Beck MW. 2017. Novel analyses of long-term data provide a scientific basis for chlorophyll-a thresholds in San Francisco Bay. Estuarine, Coastal and Shelf Science, 197:107–118.

679 Thompson JK, Koseff JR, Monismith SG, Lucas LV. 2008. Shallow water processes govern
680   system-wide phytoplankton bloom dynamics: A field study. Journal of Marine Systems,
681   74(1-2):153–166.

682 Thompson SE, Basu NB, Jr. JL, Aubeneau A, Rao PSC. 2011. Relative dominance of hydrologic
683   versus biogeochemical factors on solute export across impact gradients. Water Resources
684   Research, 47(10):W00J05.

685 Tobin J. 1958. Estimation of relationships for limited dependent variables. Econometrica,
686   26(1):24–36.

687 Wan Y, Wan L, Li Y, Doering P. 2017. Decadal and seasonal trends of nutrient concentration and
688   export from highly managed coastal catchments. Water Research, 115:180–194.

689 Wright SA, Schoellhamer DH. 2004. Trends in the sediment yield of the Sacramento River,
690   California, 1957-2001. San Francisco Estuary and Watershed Science, 2(2):1–14.

691 Zhang Q, Harman CJ, Ball WP. 2016. An improved method for interpretation of riverine
692   concentration-discharge relationships indicates long-term shifts in reservoir sediment trapping.
693   Geophysical Research Letters, 43(10):215–224.
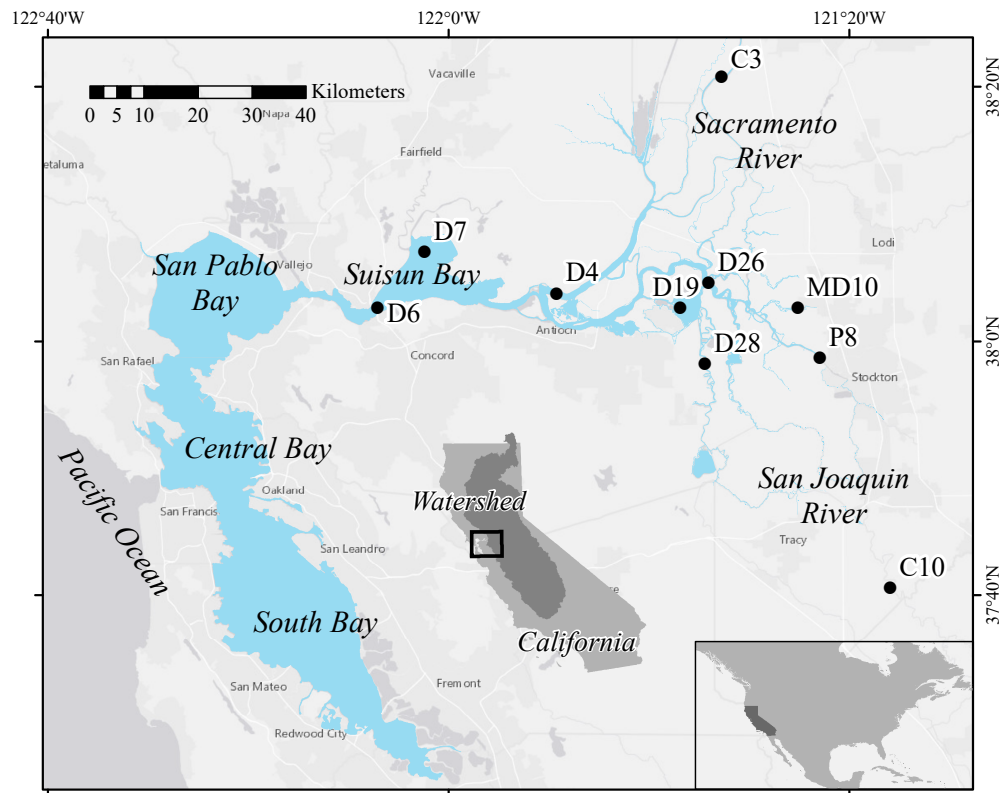
Fig. 1: The San Francisco Estuary and Delta region with monitoring stations used for analysis. The Delta drains the combined watersheds of the Sacramento and San Joaquin rivers (inset). All data were obtained from the Interagency Ecological Program website (http://water.ca.gov/bdma/meta/Discrete/data.cfm, IEP (2013)). See Table 1 for station descriptions.

`fig:delt_map`
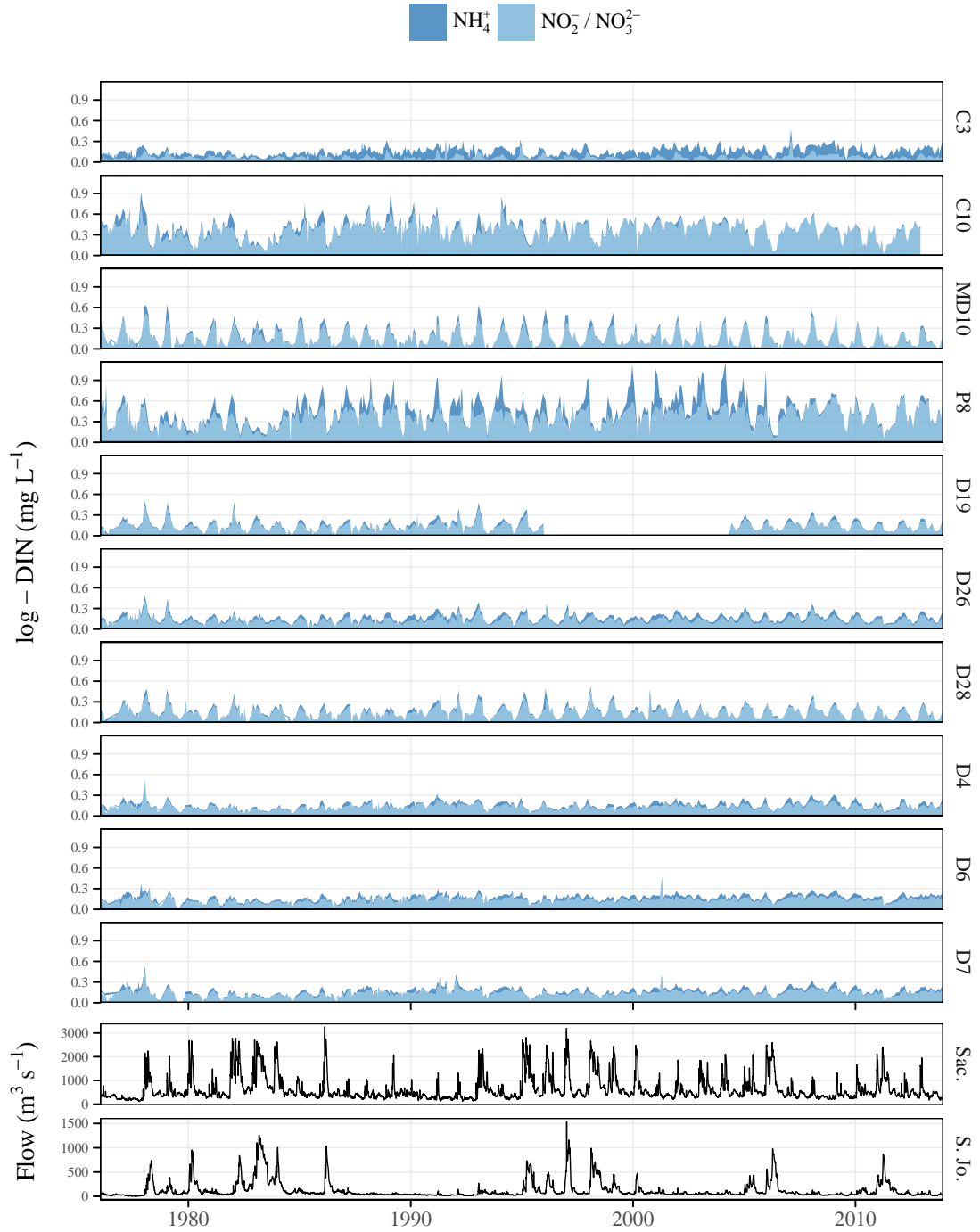
Fig. 2: Observed DIN ($NH_4^+ + NO_2^-/NO_3^{2-}$) from ten stations in the upper SFE Delta and flow from the Sacramento and San Joaquin rivers. Data were collected monthly and evaluated with WRTDS models using daily flow estimates from 1976 to 2013. Note different y-axis scales. See Fig. 1 for station locations.

fig:obsdat

Fig. 3: Model predictions for ten stations grouped by nitrogen analyte and geographic location in the Delta region (locations in Fig. 1). Results are annually-averaged for each water year from October to September. Points are model predictions and lines are flow-normalized predictions.

fig:prddat
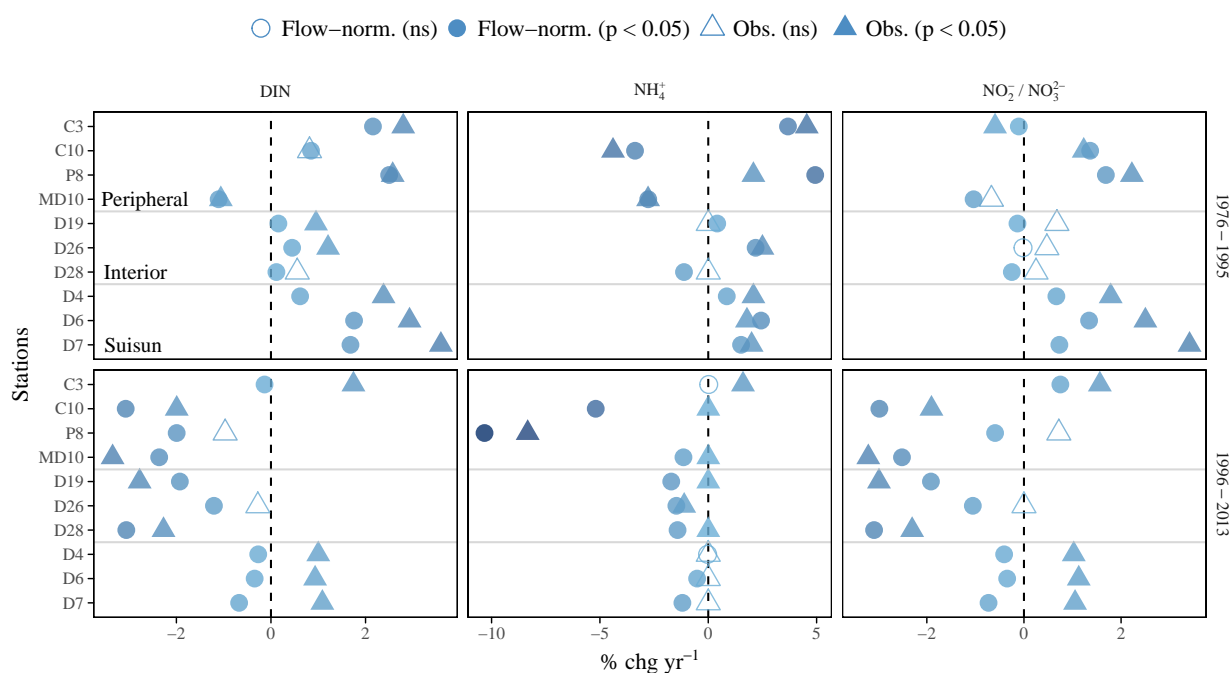
Fig. 4: Results from seasonal Kendall tests on observed data (triangles) and flow-normalized predictions (circles) from WRTDS for nitrogen analytes. Results are shown as the percent change per y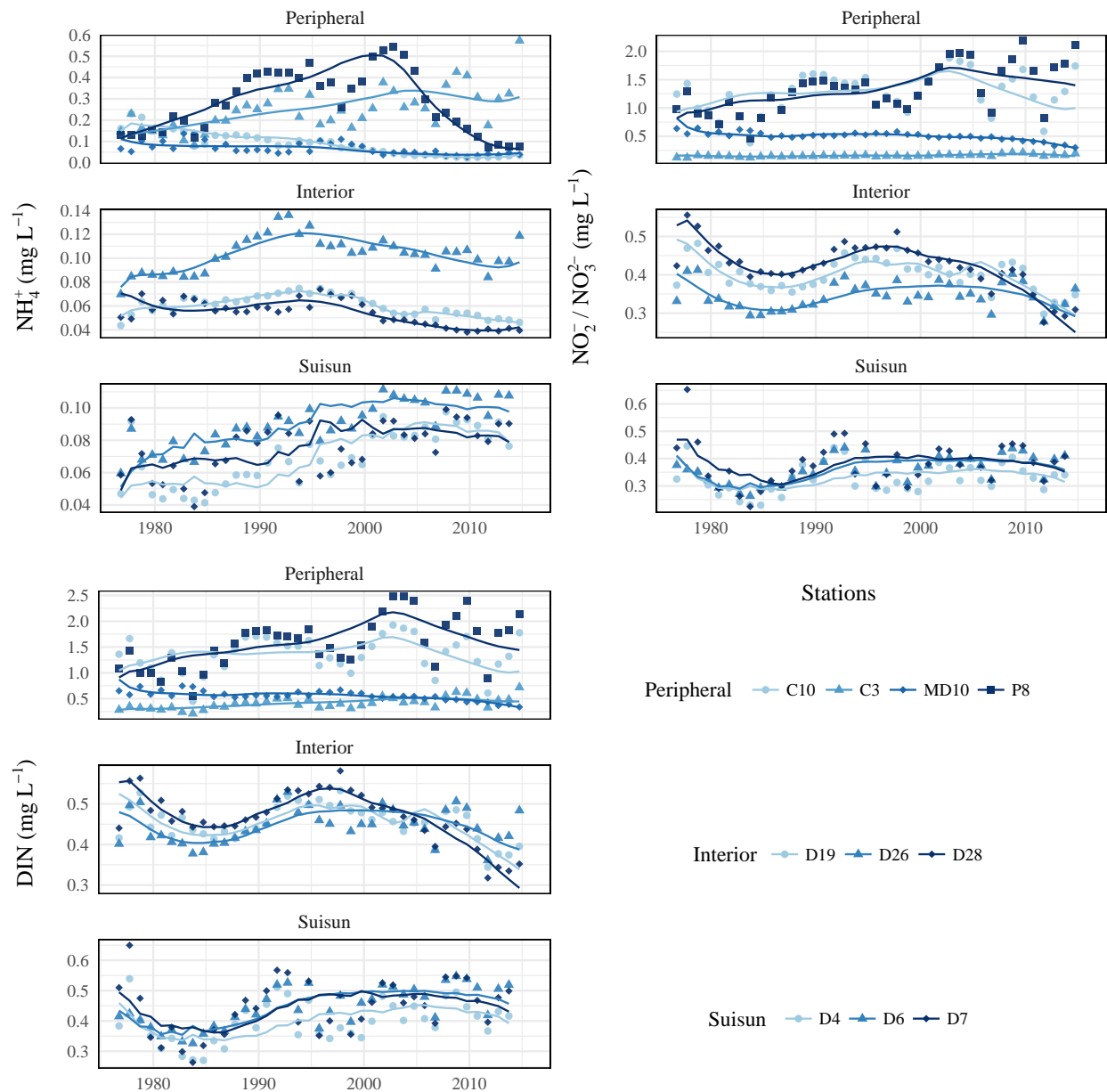ear as the estimated Theil-Sen slope divided by the median for a given aggregation period (significance evaluated at $\alpha = 0.05$, based on τ). Trends are shown separately for different annual groupings. See Figs. S1 and S2 for seasonal groupings. `fig:trndcomp1`
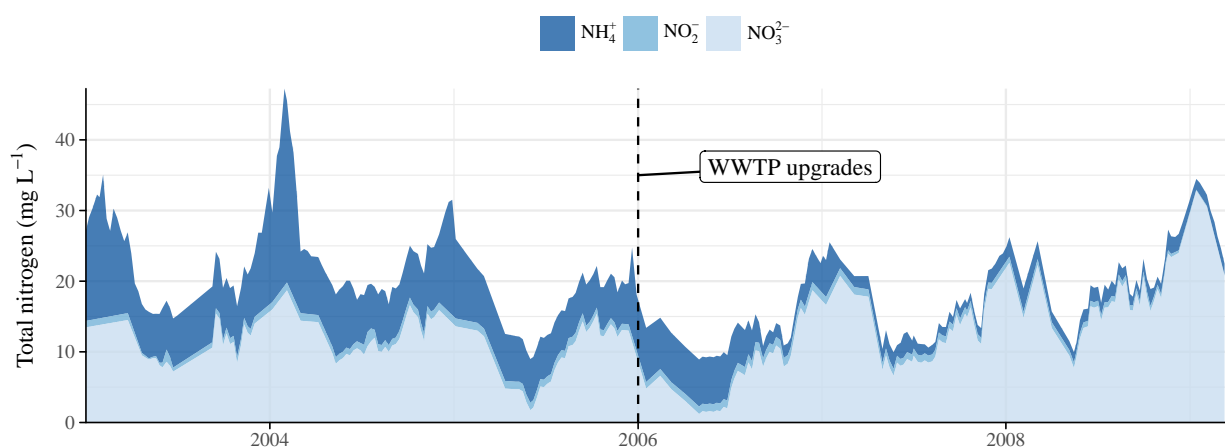
Fig. 5: Nitrogen concentration measurements (mg L^{-1}) from the City of Stockton Wastewater Treatment Plant, San Joaquin County. Wastewater discharge requirements were implemented in 2006 for nitrification/denitrification and tertiary filtration to convert ammonium to nitrate. `fig:stock`
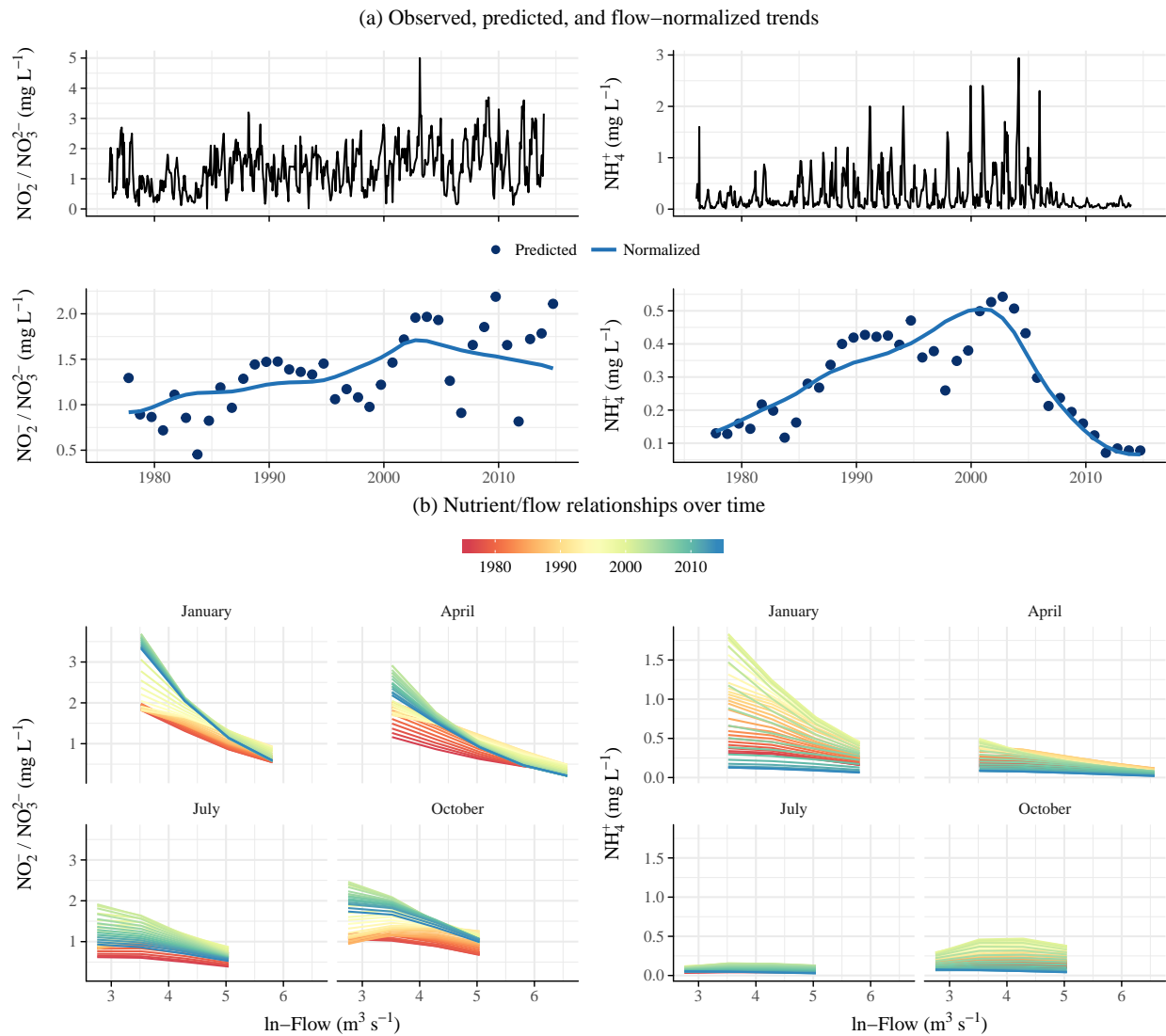
Fig. 6: Nitrogen trends at P8 as (a, top) observed, (a, bottom) predicted and flow-normalized estimates from WRTDS, and (b) relationships with flow over time from WRTDS. Nitrite/nitrate trends are on the left and ammonium trends are on the right. Wastewater treatment plant upgrades at the City of Stockton (San Joaquin County) were completed in 2006 (Fig. 5).   `fig:p8trnds`
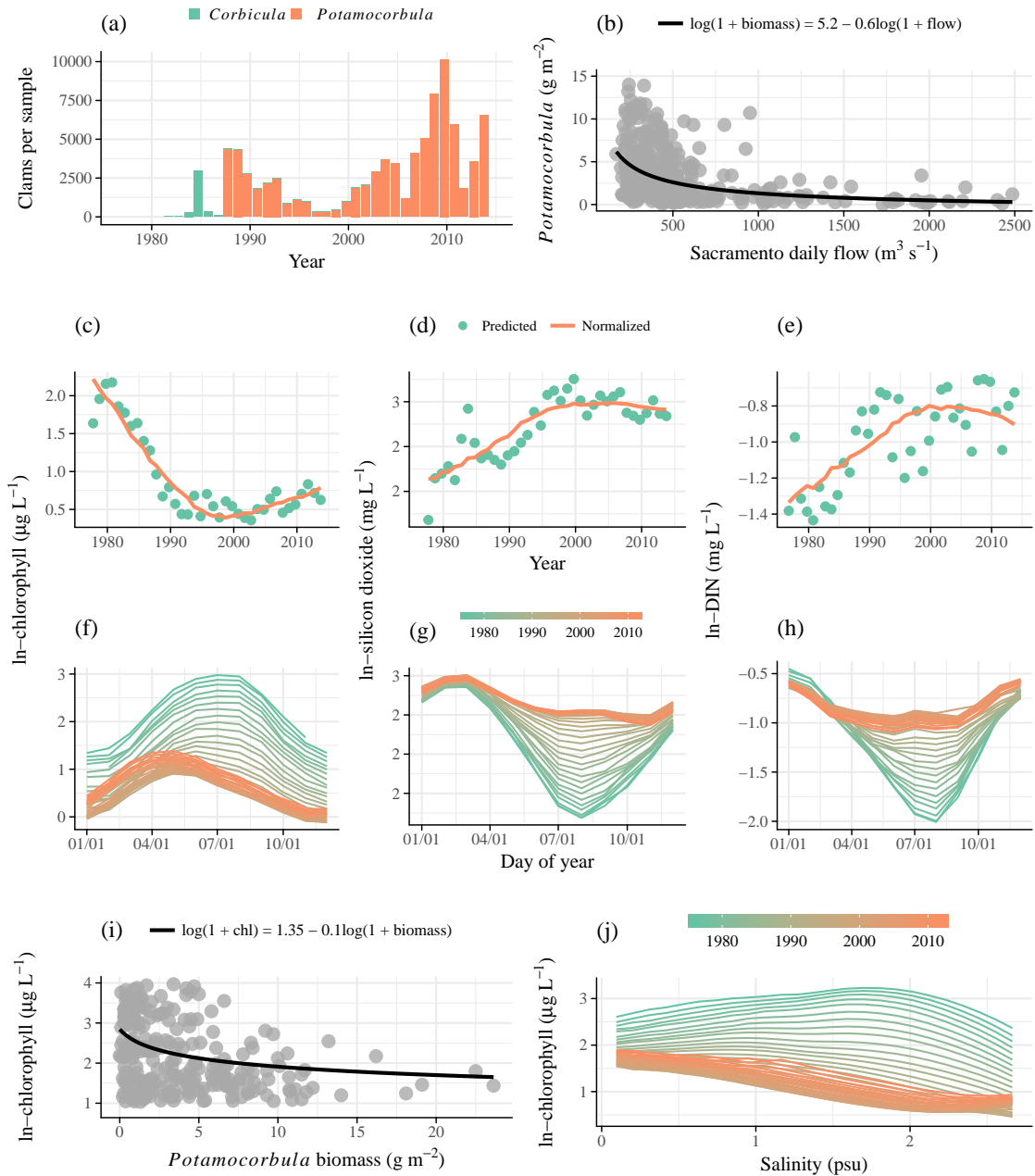
Fig. 7: Trends in clam abundance and chl-*a* concentration from 1976 to 2013 at station D7 in Suisun Bay. Invasion by *Potamocorbula amurensis* clams in the late 1980s and reduction of *Corbicula fluminea* was shown by changes in clam density (a, annual means), with biomass linked to salinity (b). A decrease in chl-*a* concentration was also observed by changes in annual (c) and seasonal trends (f) based on WRTDS results. Reductions in chl-*a* concentration were coincident with an increase in SiO_2 and DIN concentrations (d, e), with the greatest increases in August (g, h). A significant ($p < 0.001$) relationship between clam biomass and chl-*a* concentration is shown in subfigure (i). Flow relationships with chl-*a* concentration shown by WRTDS have also changed over time (j, observations from June).

fig:clmchl

36

Table 1: Monitoring stations in the upper San Francico Estuary used to evaluate nitrogen trends. Records from 1976 to 2013 were evaluated using the total observations (n) at each station. Median values are reported in mg L^{-1}. tab:stdescrp

Station	Lat	Lon	DIN		NH$_4^+$		NO$_2^-$/NO$_3^{2-}$	
			n	Med.	n	Med.	n	Med.
Peripheral								
C3	38.35	-121.55	569	0.36	569	0.22	571	0.13
C10	37.68	-121.27	539	1.44	539	0.04	558	1.40
MD10	38.04	-121.42	548	0.31	548	0.03	570	0.28
P8	37.98	-121.38	556	1.46	556	0.12	563	1.20
Interior								
D19	38.04	-121.61	433	0.35	435	0.04	462	0.31
D26	38.08	-121.57	556	0.38	556	0.09	565	0.29
D28	37.97	-121.57	529	0.38	535	0.03	555	0.33
Suisun								
D4	38.06	-121.82	546	0.38	546	0.05	565	0.32
D6	38.04	-122.12	534	0.45	534	0.08	562	0.35
D7	38.12	-122.04	535	0.44	535	0.06	561	0.36

Table 2: Summaries of flow-normalized trends in nitrogen analytes for all stations and annual aggregations tab:trndsann

Analyte/Station	Annual	
	1976-1995	1996-2013
DIN		
C10	1.3 (**0.8**)*	1.4 (-3.1)*
C3	0.3 (**2.2**)*	0.5 (-0.1)*
D19	0.4 (**0.2**)*	0.4 (-1.9)*
D26	0.4 (**0.4**)*	0.5 (-1.2)*
D28	0.4 (**0.1**)*	0.4 (-3.1)*
D4	0.3 (**0.6**)*	0.4 (-0.3)*
D6	0.4 (**1.8**)*	0.5 (-0.3)*
D7	0.4 (**1.7**)*	0.5 (-0.7)*
MD10	0.4 (-1.1)*	0.3 (-2.4)*
P8	1.3 (**2.5**)*	1.7 (-2)*
NH_4^+		
C10	0.1 (-3.4)*	0 (-5.2)*
C3	0.2 (**3.7**)*	0.3 (**0**)
D19	0 (**0.4**)*	0 (-1.7)*
D26	0.1 (**2.2**)*	0.1 (-1.5)*
D28	0 (-1.1)*	0 (-1.4)*
D4	0 (**0.9**)*	0.1 (**0**)
D6	0.1 (**2.4**)*	0.1 (-0.5)*
D7	0.1 (**1.5**)*	0.1 (-1.2)*
MD10	0.1 (-2.8)*	0 (-1.1)*
P8	0.2 (**4.9**)*	0.1 (-10.3)*
NO_2^-/NO_3^{2-}		
C10	1.2 (**1.4**)*	1.4 (-3)*
C3	0.1 (-0.1)*	0.2 (**0.7**)*
D19	0.4 (-0.1)*	0.4 (-1.9)*
D26	0.3 (**0**)	0.4 (-1.1)*
D28	0.4 (-0.2)*	0.4 (-3.1)*
D4	0.3 (**0.7**)*	0.3 (-0.4)*
D6	0.3 (**1.3**)*	0.4 (-0.3)*
D7	0.4 (**0.7**)*	0.4 (-0.7)*
MD10	0.4 (-1)*	0.3 (-2.5)*
P8	1.2 (**1.7**)*	1.5 (-0.6)*

Summaries are medians (mg L^{-1}) and percent change per year in parentheses (increasing in bold). Changes and significance estimates are based on seasonal Kendall tests of flow-normalized results within each time period. *$p <$ 0.05

Table 3: Summaries of flow-normalized trends in nitrite/nitrate and ammonium (mg L^{-1}) concentrations before and after WWTP upgrades upstream of station P8 tab:p8chg

Period	NO_2^-/NO_3^{2-}		NH_4^+	
	Median	% change	Median	% change
Annual				
1976-2006	1.3	**2***	0.2	**2.8***
2007-2013	1.4	-1.9*	0.1	-16.6*
Seasonal, pre				
Spring	1.2	**1.6***	0.2	**1.4***
Summer	1	**2.4***	0.1	**3.3***
Fall	1.3	**2.2***	0.2	**4.9***
Winter	1.5	**2.1***	0.7	**4.8***
Seasonal, post				
Spring	1.3	-1.6*	0.1	-16.2*
Summer	0.9	-4.3*	0.1	-15.7*
Fall	1.5	-1.7*	0.1	-19.3*
Winter	2.2	-0.8*	0.2	-26.7*

Upgrades were completed in 2006 at the City of Stockton WWTP (San Joaquin County, Fig. 5). Summaries are medians and percent change per year in parentheses (increasing in bold). Changes and significance estimates are based on seasonal Kendall tests of flow-normalized results within each time period. Increasing values are in bold-italics. Months for each season are Spring: MAM, Summer: JJA, Fall: SON, Winter: DJF. *$p < 0.05$

Fig. S1: Results from seasonal Kendall tests on observed data (triangles) and flow-normalized predictions (circles) from WRTDS for nitrogen analytes. Results are shown as the percent change per year as the estimated Theil-Sen slope divided by the median for a given aggregation period (significance evaluated at $\alpha = 0.05$, based on τ). Trends are shown separately for different seasonal groupings from 1976-1995. Months for each season are Spring: MAM, Summer: JJA, Fall: SON, Winter: DJF. See Fig. 4 for annual comparisons.
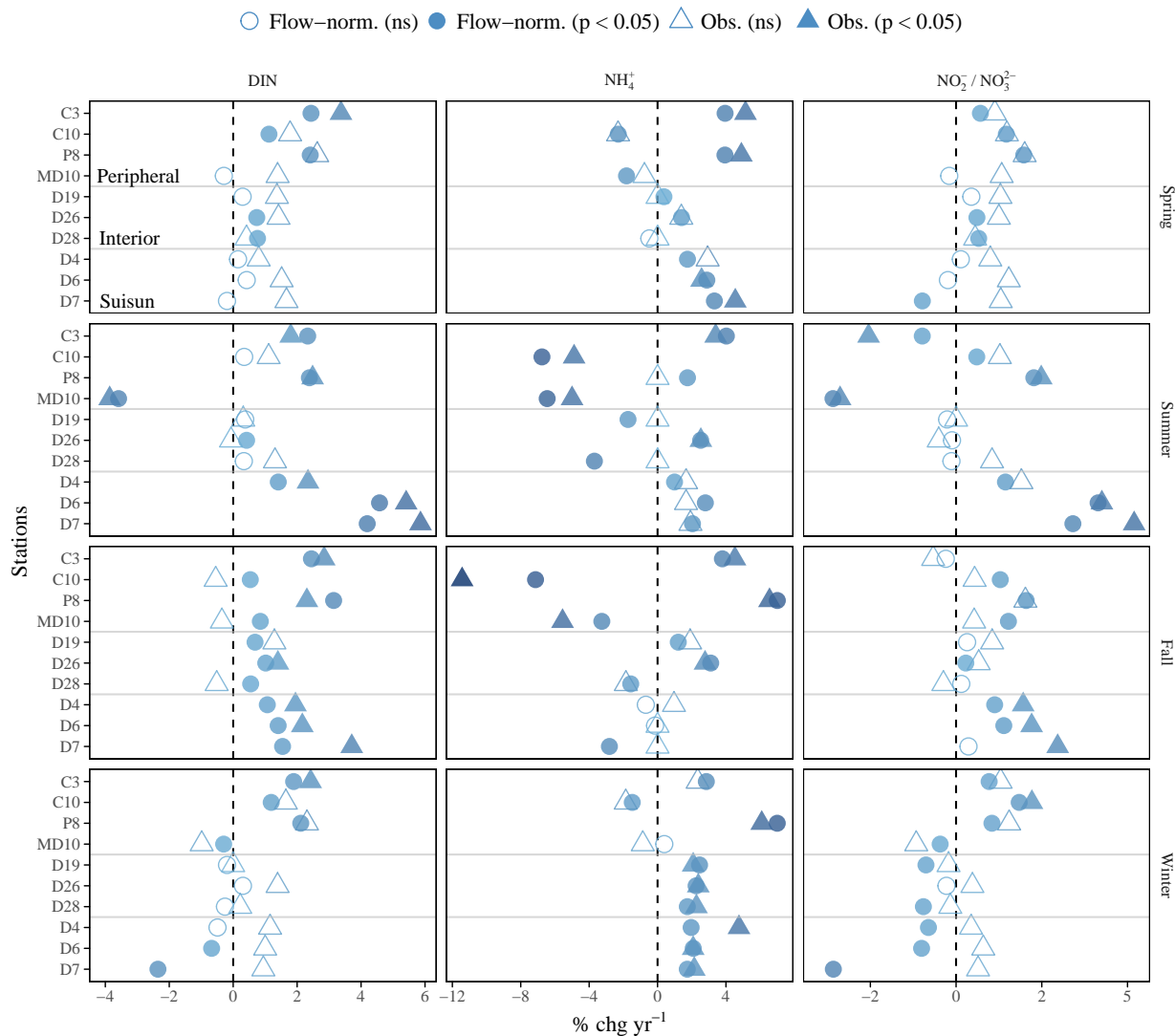
fig:trndcomp2

Fig. S2: Results from seasonal Kendall tests on observed data (triangles) and flow-normalized predictions (circles) from WRTDS for nitrogen analytes. Results are shown as the percent change per year as the estimated Theil-Sen slope divided by the median for a given aggregation period (significance evaluated at $\alpha = 0.05$, based on τ). Trends are shown separately for different seasonal groupings from 1996-2013. Months for each season are Spring: MAM, Summer: JJA, Fall: SON, Winter: DJF. See Fig. 4 for annual comparisons.
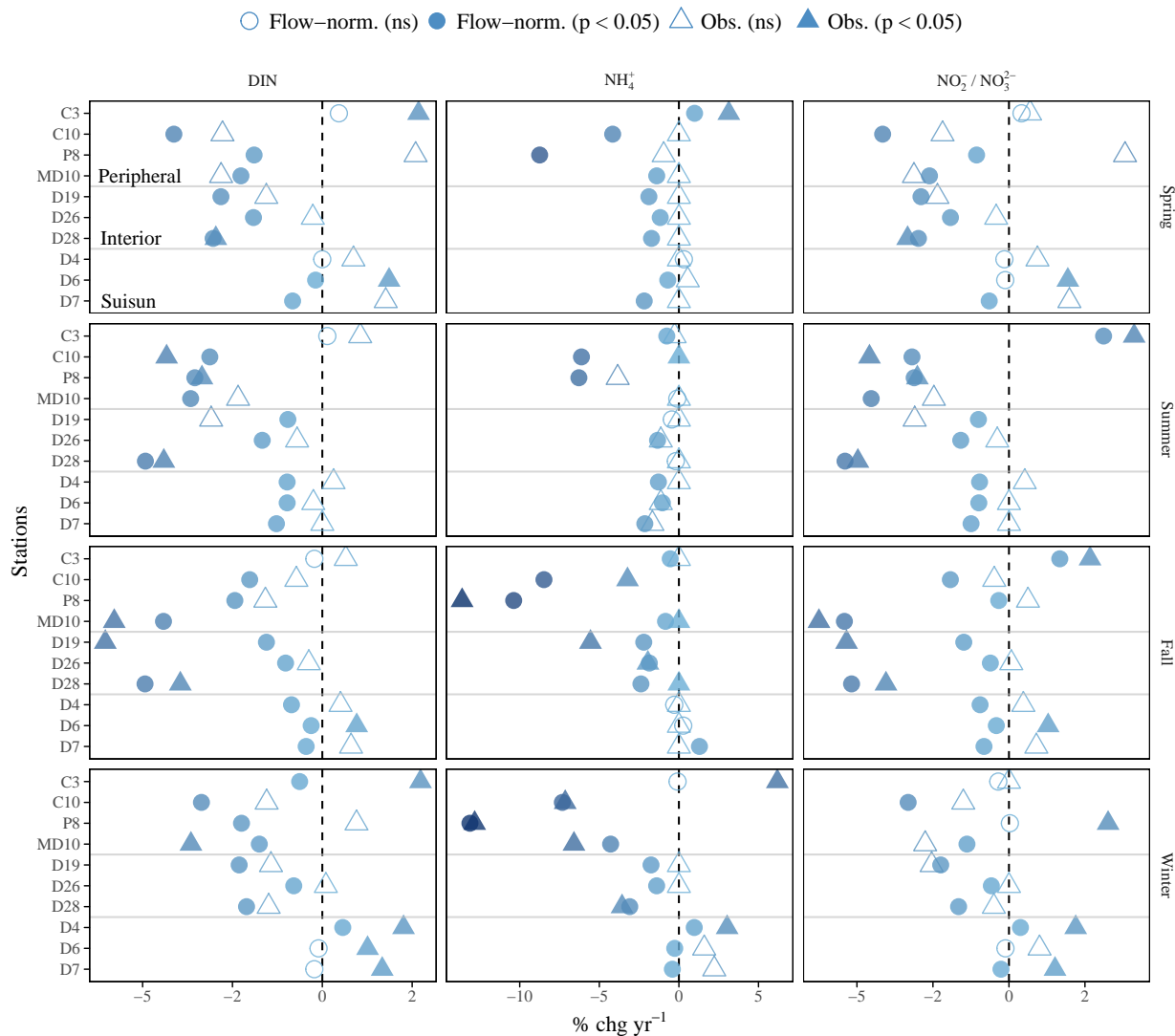
fig:trndcomp3

Table S1: Summaries of flow-normalized trends in nitrogen analytes for all stations and seasonal aggregations from 1976-1995 tab:trndsbef

Analyte/Station	Seasonal, 1976-1995			
	Spring	Summer	Fall	Winter
DIN				
C10	1.2 (**1.1**)*	1.2 (**0.3**)	1.3 (**0.5**)*	1.7 (**1.2**)*
C3	0.3 (**2.4**)*	0.3 (**2.3**)*	0.4 (**2.4**)*	0.4 (**1.9**)*
D19	0.5 (**0.3**)	0.2 (**0.4**)	0.3 (**0.7**)*	0.7 (-0.2)
D26	0.4 (**0.7**)*	0.3 (**0.4**)*	0.4 (**1**)*	0.6 (**0.3**)
D28	0.5 (**0.8**)*	0.2 (**0.3**)	0.3 (**0.5**)*	0.8 (-0.3)
D4	0.4 (**0.2**)	0.3 (**1.4**)*	0.3 (**1.1**)*	0.5 (-0.5)
D6	0.4 (**0.4**)	0.3 (**4.6**)*	0.4 (**1.4**)*	0.5 (-0.7)*
D7	0.4 (-0.2)	0.3 (**4.2**)*	0.4 (**1.5**)*	0.6 (-2.4)*
MD10	0.6 (-0.3)	0.2 (-3.6)*	0.3 (**0.8**)*	1.3 (-0.3)*
P8	1.3 (**2.4**)*	0.9 (**2.4**)*	1.3 (**3.1**)*	1.9 (**2.1**)*
NH$_4^+$				
C10	0.1 (-2.3)*	0 (-6.8)*	0.1 (-7.1)*	0.3 (-1.5)*
C3	0.2 (**3.9**)*	0.2 (**4**)*	0.3 (**3.8**)*	0.2 (**2.9**)*
D19	0.1 (**0.4**)*	0 (-1.7)*	0 (**1.2**)*	0.1 (**2.5**)*
D26	0.1 (**1.4**)*	0.1 (**2.5**)*	0.1 (**3.1**)*	0.1 (**2.3**)*
D28	0.1 (-0.5)	0 (-3.7)*	0 (-1.6)*	0.1 (**1.7**)*
D4	0.1 (**1.7**)*	0 (**1**)*	0 (-0.7)	0.1 (**2**)*
D6	0.1 (**2.9**)*	0.1 (**2.8**)*	0.1 (-0.1)	0.1 (**2.1**)*
D7	0.1 (**3.3**)*	0 (**2**)*	0.1 (-2.8)*	0.1 (**1.7**)*
MD10	0.1 (-1.8)*	0 (-6.5)*	0 (-3.3)*	0.2 (**0.4**)
P8	0.2 (**3.9**)*	0.1 (**1.8**)*	0.2 (**7**)*	0.6 (**7**)*
NO$_2^-$/NO$_3^{2-}$				
C10	1.1 (**1.5**)*	1.2 (**0.6**)*	1.2 (**1.3**)*	1.5 (**1.8**)*
C3	0.2 (**0.7**)*	0.1 (-1)*	0.1 (-0.3)	0.2 (**1**)*
D19	0.4 (**0.4**)	0.2 (-0.3)	0.3 (**0.3**)	0.6 (-0.9)*
D26	0.4 (**0.6**)*	0.2 (-0.1)	0.3 (**0.3**)*	0.5 (-0.3)
D28	0.5 (**0.7**)*	0.2 (-0.1)	0.3 (**0.2**)	0.7 (-1)*
D4	0.3 (**0.1**)	0.3 (**1.4**)*	0.3 (**1.1**)*	0.4 (-0.8)*
D6	0.4 (-0.2)	0.3 (**4.1**)*	0.3 (**1.4**)*	0.4 (-1)*
D7	0.4 (-1)*	0.3 (**3.4**)*	0.4 (**0.4**)	0.4 (-3.6)*
MD10	0.5 (-0.2)	0.2 (-3.6)*	0.2 (**1.5**)*	1.2 (-0.5)*
P8	1.2 (**2**)*	0.9 (**2.3**)*	1.1 (**2**)*	1.4 (**1**)*

Summaries are medians (mg L^{-1}) and percent change per year in parentheses (increasing in bold). Changes and significance estimates are based on seasonal Kendall tests of flow-normalized results within each time period. Months for each season are Spring: MAM, Summer: JJA, Fall: SON, Winter: DJF. *$p < 0.05$

Table S2: Summaries of flow-normalized trends in nitrogen analytes for all stations and seasonal aggregations from 1996-2013 tab:trndsaft

Analyte/Station	Seasonal, 1996-2013			
	Spring	Summer	Fall	Winter
DIN				
C10	1.1 (-4.1)*	1.3 (-3.1)*	1.6 (-2)*	1.7 (-3.4)*
C3	0.5 (**0.5**)	0.4 (**0.1**)	0.6 (-0.2)	0.5 (-0.6)*
D19	0.5 (-2.8)*	0.2 (-1)*	0.3 (-1.6)*	0.7 (-2.3)*
D26	0.5 (-1.9)*	0.3 (-1.7)*	0.4 (-1)*	0.6 (-0.8)*
D28	0.5 (-3)*	0.2 (-4.9)*	0.2 (-4.9)*	0.7 (-2.1)*
D4	0.4 (**0**)	0.4 (-1)*	0.4 (-0.9)*	0.5 (**0.6**)*
D6	0.5 (-0.2)*	0.5 (-1)*	0.5 (-0.3)*	0.5 (-0.1)
D7	0.5 (-0.8)*	0.4 (-1.3)*	0.4 (-0.4)*	0.6 (-0.2)
MD10	0.4 (-2.3)*	0.2 (-3.7)*	0.2 (-4.4)*	1 (-1.8)*
P8	1.5 (-1.9)*	1.2 (-3.5)*	1.8 (-2.4)*	2.7 (-2.2)*
NH_4^+				
C10	0 (-4.2)*	0 (-6.1)*	0 (-8.5)*	0.1 (-7.3)*
C3	0.3 (**1**)*	0.3 (-0.8)*	0.4 (-0.5)*	0.2 (-0.1)
D19	0 (-1.9)*	0 (-0.4)	0 (-2.2)*	0.1 (-1.8)*
D26	0.1 (-1.2)*	0.1 (-1.3)*	0.1 (-1.9)*	0.1 (-1.4)*
D28	0 (-1.7)*	0 (-0.2)	0 (-2.4)*	0.1 (-3.1)*
D4	0.1 (**0.3**)	0 (-1.3)*	0.1 (-0.3)	0.1 (**1**)*
D6	0.1 (-0.7)*	0.1 (-1)*	0.1 (**0.3**)	0.1 (-0.3)*
D7	0.1 (-2.2)*	0 (-2.1)*	0.1 (**1.3**)*	0.1 (-0.4)*
MD10	0 (-1.4)*	0 (-0.1)	0 (-0.8)*	0.1 (-4.3)*
P8	0.2 (-8.7)*	0.1 (-6.3)*	0.2 (-10.4)*	0.5 (-13.1)*
NO_2^-/NO_3^{2-}				
C10	1.1 (-4.2)*	1.2 (-3.2)*	1.6 (-1.9)*	1.6 (-3.3)*
C3	0.2 (**0.4**)	0.1 (**3.1**)*	0.2 (**1.7**)*	0.2 (-0.4)
D19	0.4 (-2.9)*	0.2 (-1)*	0.3 (-1.5)*	0.6 (-2.2)*
D26	0.4 (-1.9)*	0.2 (-1.6)*	0.3 (-0.6)*	0.5 (-0.6)*
D28	0.5 (-3)*	0.2 (-5.4)*	0.2 (-5.2)*	0.7 (-1.7)*
D4	0.3 (-0.1)	0.3 (-1)*	0.3 (-1)*	0.4 (**0.4**)*
D6	0.4 (-0.1)	0.4 (-1)*	0.4 (-0.4)*	0.4 (-0.1)
D7	0.4 (-0.6)*	0.4 (-1.2)*	0.4 (-0.8)*	0.4 (-0.3)*
MD10	0.4 (-2.6)*	0.1 (-4.5)*	0.2 (-5.4)*	1 (-1.4)*
P8	1.3 (-1.1)*	1.1 (-3.1)*	1.6 (-0.3)*	2.2 (**0**)

Summaries are medians (mg L^{-1}) and percent change per year in parentheses (increasing in bold). Changes and significance estimates are based on seasonal Kendall tests of flow-normalized results within each time period. Months for each season are Spring: MAM, Summer: JJA, Fall: SON, Winter: DJF. *$p < 0.05$